Building and Environment 60 (2013) 116–125

Contents lists available at SciVerse ScienceDirect

Building and Environment

journal homepage: www.elsevier.com/locate/buildenv

Numerical investigation of particle transport and inhalation using standing thermal manikins

Xiangdong Li [a], Kiao Inthavong [a], Qinjiang Ge [a], Jiyuan Tu [a,b,*]

[a] School of Aerospace, Mechanical and Manufacturing Engineering, RMIT University, PO Box 71, Plenty Road, Bundoora VIC 3083, Australia
[b] Institute of Nuclear and New Energy Technology, Tsinghua University, PO Box 1021, Beijing 100084, China

ARTICLE INFO

Article history:
Received 12 October 2012
Received in revised form
22 November 2012
Accepted 27 November 2012

Keywords:
Body posture
Heat transfer
Particle transport
Particle inhalation
Critical area

ABSTRACT

Our previous study [1] demonstrated that for a thermal manikin in a horizontal airflow, its orientation relative to the free stream has a significant effect on the characteristics of particle transport and inhalation. Based on this conclusion, the previous research [1] was extended and the effect of leg posture (e.g. combined legs and divided legs) on particle inhalation in horizontal free stream was investigated using Computational Fluid Dynamics (CFD) in this study. The numerical results agreed well the experimental data and empirical correlations in the literature. It was revealed that for an occupant standing with its back towards the horizontal airflow, a little change in the leg posture can lead to an obvious variation in the source location of inhaled particles. It was also found that different leg postures have different environment sensitivity since when the manikin legs are divided, the central height of the critical area does not obviously change with increasing wind speed, however, this central height increases significantly with the wind speed when the legs are combined.

1. Introduction

The human thermal plume, which is the buoyancy-driven convection in the vicinity of a human body induced by the human metabolic heat, has been recognized as an important role in affecting indoor air quality (IAQ) and thermal comfort. Experimental evidences [2–4] demonstrated that the human thermal plume can produce a vertical air velocity up to 0.25 m/s in quiescent air, which is roughly equal to the average wind speed in most modern indoor environments (0.05–0.25 m/s according to Baldwin and Maynard [5]). Furthermore, thanks to the rapid development of low-power office/home devices such as LCD screens and halogen lamps, it is believed that the thermal plume generated by the occupants would be the major thermal flows in a future indoor environment [6]. Therefore, it is reasonable to expect that the thermal plume may obviously affect the airflow pattern in the vicinity of a human body and play an important role in pollutant transport in indoor environments.

In recent years, with increasing awareness of the hazards caused by particulate contaminants (e.g. PM2.5), the role of thermal plume in transporting aerosol particles in indoor environments, especially in the vicinity of the human occupants, has become an important research interest. Rim and Novoselac [7] measured the particle concentration around a breathing thermal manikin seated in quasi-quiescent air. It was found that due to the entraining effect of thermal plume on aerosol particles, the inhaled particle concentrations were up to 4 times higher than the ambient concentrations when the particle source was located at floor level and in near proximity to the manikin. This indicated that the thermal plume plays an important role in transporting pollutants from the floor level into the breathing zone. However, the practical situations are much more complicated since the thermal plume around a human occupant is subjected to many factors such as the indoor airflow pattern and temperature, furniture layout, as well as personal factors including activity level, body posture, clothing design and even the level of baldness [6]. Any factor that may have an effect on the thermal plume is expected to indirectly change the characteristics of particle transport and inhalation. This is especially true for fine and ultrafine particles as their movement is mostly controlled by the airflow field [8].

Among these factors, the orientation of an occupant relative to the ventilating airflow, which may be affected by the ventilation system layout and the occupant location in a room, is an important

* Corresponding author. School of Aerospace, Mechanical and Manufacturing Engineering, RMIT University, PO Box 71, Bundoora VIC 3083, Australia. Tel.: +61 3 9925 6191; fax: +61 3 9925 6108.
E-mail address: jiyuan.tu@rmit.edu.au (J. Tu).

0360-1323/$ – see front matter © 2012 Elsevier Ltd. All rights reserved.
http://dx.doi.org/10.1016/j.buildenv.2012.11.014

one. Due to the limitation of the extreme complexity, horizontal airflow was widely assumed in previous studies [1,9,10] to simplify the issue. A CFD computation by Hyun and Kleinstreuer [10] revealed that for an occupant standing in a horizontal free stream, the concentration of inhaled pollutant is jointly influenced by the location of pollutant source and the occupant orientation. A recent CFD investigation by the authors [1] further proved that when an occupant is back-to-the-wind oriented in a horizontal airflow, its breathing zone is located in the thermal plume region which is on the downstream side of the occupant and the characteristics of particle inhalation are highly impacted by the body heat.

Apart from this, the body posture seems to be another important factor which deserves a great importance. The experimental measurements by Kurazumi et al.'s [11] demonstrated that the body posture has a significant effect on the heat transfer coefficient between a human body and its surroundings, which hence leads to different thermal flow intensity around the human body. In addition, Hayashi et al. [12] conducted a numerical investigation of contaminant inhalation through the mouth in a displacement ventilated environment. Thermal manikins with different body postures including standing, sitting and lying were studied. It was found that when an occupant is standing or seated, the inhaled air is delivered from the area close to the floor and then drawn upward into the breathing zone by the thermal plume. However, when the occupant is lying, the thermal plume seems to have no significant effect since the inhalation region extends horizontally out from the head. These experimental and numerical evidences indicate that the body posture may have a significant effect on the pollutant transport and inhalation characteristics in the vicinity of a human body through affecting the thermal plume. Unfortunately, due to the extreme complexity, the effects of body posture on particle transport and inhalation under a thermal flow condition have not been thoroughly understood and further research is still in need.

Therefore, based on the research outcomes yielded from our previous study [1], this study is aimed to investigate the effects of body posture on particle transport around and particle inhalation by a thermal manikin standing in a horizontal free steam. The low-speed horizontal wind tunnel and its boundary setup as shown in Reference [1] were adopted in this study. Two thermal manikins with slightly different body postures were employed, namely one standing with its legs combined together while the other standing with its legs divided. Based on the conclusion risen from our previous study [1] that the thermal plume has no detectable effects on particle inhalation when the manikin is facing-the-wind, the manikins were arranged to be back-to-the-wind. For the purpose of comparison, computations were also conducted with the isothermal conditions. This study not only demonstrated that a little change in the leg posture may lead to a significant difference in the particle transport and inhalation characteristics, it also indicated that different body postures have different environment sensitivity. This may be of a great importance when assessing the environment hazards associated with particle inhalation and to find out an optimal body posture to avoid them.

2. Numerical methods

2.1. The thermal manikins

The thermal plume actually develops along the body surface from the lowest body segments such as the feet. Therefore, the layout of the heat-releasing body segments lower than the breathing zone may have significant effects on the thermal plume and particle transport into the breathing zone. Among them, the legs seem to have important impact. Brohus and Nielsen [13] suggested that for a CFD simulation of airflow around a standing manikin in a low velocity space, it is important to include legs in the simulation so that the transport path of contaminants could be effectively simulated. In most of the previous CFD simulations of airflow around a standing manikin, the two legs were usually assumed to be combined together and the gap between legs was neglected [9,14]. However, a numerical simulation by Hyun and Kleinstreuer [10] using a standing CTM with divided legs presented a totally different airflow pattern in the vicinity of the manikin from that in Reference [9] which employed a combined-leg manikin. Gao and Niu [15] summarized that if the human body faces a horizontal airflow, the gap between the legs will allow air to flow across the lower body and affect the entrainment of rising airflow which therefore affects the contaminant concentration at the breathing level.

Therefore, in order that the effects of leg posture on particle inhalation could be clarified, two slightly different thermal manikins were employed in this study, as illustrated in Fig. 1. The two manikins have exactly the same upper body segments while slightly different leg segments. One manikin stands with its legs combined (Fig. 1(a)) and the other stands with it legs divided (Fig. 1(b)), which allows a gap of 0.0488 m^2 between the legs. The difference in the legs leads to slightly different surface areas of the manikins, which are 1.329 m^2 for the combined-leg one and 1.394 m^2 for the divided-leg one, respectively. In addition, for the dual purposes of an improved prediction accuracy in the breathing zone and a reduced computational cost as recommended by Gao and Niu [15], the manikin heads were carefully created based on the anthropometric data of Tilley [16] while the other body segments are simplified as blocks.

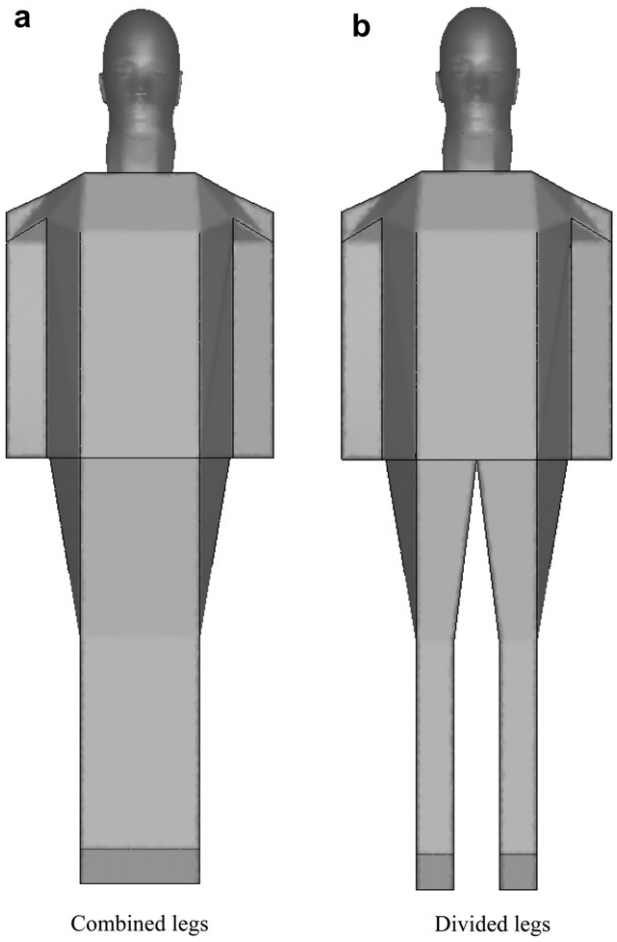

Fig. 1. Computational thermal manikins employed in this study..

2.2. Boundary conditions and numerical procedures

The horizontal wind tunnel (4 m-width × 7 m-depth × 3 m-height) and its airflow conditions (26 °C evenly distributed horizontal free stream with different speed of 0.05, 0.10, 0.15, 0.20 and 0.25 m/s, respectively) which were highlighted in our previous study [1] are continued to be employed in this study. The tunnel walls were assumed to be adiabatic. The manikins shown in Fig. 1 were oriented in the tunnel with their backs facing the free stream, respectively, with one manikin for one computation. The manikin was also properly placed with its nose tip located in the$X = 0$plane, as shown in Fig. 2. For inhalation simulation, the periodic respiration was neglected and a constant inhalation rate of 15 L per minute (LPM) representing a human light breath at light activity conditions was equally applied at the manikin nostrils, namely 7.5 LPM for each nostril. The validity of steady state assumption has been discussed in our previous study [19] and is not repeated here. For heat transfer modelling between the manikin and its environment, the heat loss caused by respiration, evaporation and radiation were ignored and only convective heat transfer was taken into account. A constant temperature of 31 °C was applied on the manikin surface, as recommended by Niu and Gao [17] as well as by Sorensen and Voigt [18]. The manikin surface temperature here is also in the human body surface temperature range available in the literature [15]. In addition, for the purpose of comparison, computations with isothermal flows were also conducted.

Particles with fixed diameter of 1.0 micron and density of 1000 kg/m^3 were released with the same speed of the free stream from a circular region with diameter of 1.6 m and located in the $X = -2$ m plane (namely 2.0 m upstream of the nose tip, Fig. 2). The particle size of 1.0 micron was selected since the transport of particles at this size is strongly controlled by the airflow field and they are therefore easy to be inhaled [19]. The particle injection region was located far enough from the nose tip plane so that the particle trajectories could be fully developed before being affected by the thermal plume. Such a big area of particle injection region could allow locating the source of inhaled particles in a wide parametric range. Computations demonstrated that the numerical results were independent of the number of particle trajectories when the trajectory number was over 50,000.

The incompressible Navier–Stokes Equations are solved for the airflow field and the particles are tracked through the airflow field separately using the Lagrangian approach. The airflow turbulence is modelled using the RNG $k-\varepsilon$ model due to its successful application in modelling indoor airflow and pollutant transport [17]. Details of the theoretical models have been highlighted elsewhere [1,19] and are not repeated here for brevity.

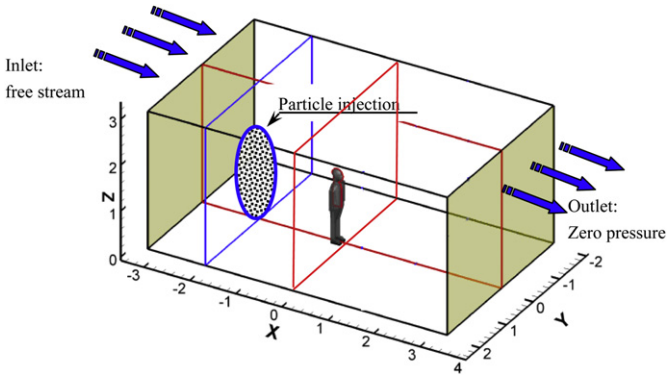

Fig. 2. Computational model setup.

The computational domain was discretized using unstructured tetrahedral and prism meshes. In order to overcome the convergence difficulty caused by the complicated manikin geometry and to capture the effects of manikin geometry on the thermal plume, 20 layers of fine inflation meshes were created around the manikin surface, as shown in Fig. 3. The grid sensitivity test proved that mesh independence was achieved at around 4.0 million cells, with the skewness of the cells and $y+$ value on the walls dropped below 0.8 and 0.78 respectively. The equations were then solved in ANSYS CFX 13 using a segregated solver with an implicit formulation. The residual values of the transport equations were set to converge at 10^{-5} or below for all simulation cases.

3. Results and discussion

3.1. Airflow field

For the purpose of quantitative comparison, air velocity distributions in 2 planes and along 4 lines are analysed. The locations of the planes and lines are illustrated in Fig. 4, where Plane 1 is a vertical XZ plane at $Y = 0$ m and Plane 2 is a horizontal XY plane at $Z = 0.43$ m. Line 1 and Line 2 are vertical lines in Plane 1, which are 0.05 m and 0.20 m downstream of the nose tip, respectively. Line 3 and Line 4 are horizontal lines in Plane 2, which are 0.05 m downstream and upstream of the legs, respectively.

Our previous study [1] demonstrated that for an occupant in a horizontal free stream, the affected region of body heat is located on the downstream side of an occupant, therefore, the occupant orientation relative to the free stream becomes an important factor deciding whether and how much the body heat has an effect on the characteristics of contaminant transport and inhalation. The overall airflow fields around a manikin [1] illustrated that when the thermal manikin is back-to-the-wind, the air and contaminant in its breathing zone is actually delivered by the thermal plume from a lower level. In this study, the airflow fields in the breathing zone of a leeward manikin under isothermal and thermal conditions were further compared, as illustrated in Fig. 5(a) and (b), respectively. It was found that when heat transfer was excluded from the CFD model, there is a significant descending airflow in front of the

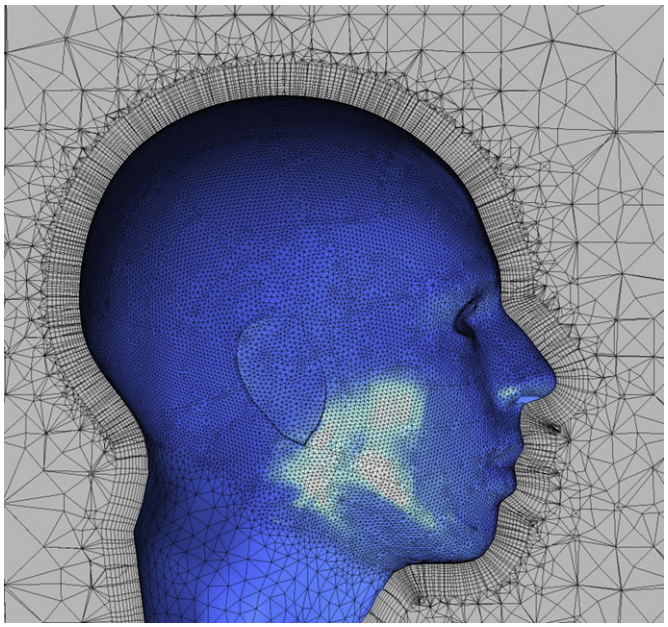

Fig. 3. Refined computational mesh around the manikin surface.

nose, which is a result of airflow passing around the manikin head from the top. The descending airflow is then partially inhaled together with the airflow ascending from a lower height. However, the inclusion of heat transfer in the CFD model presents a totally different airflow field, as illustrated in Fig. 5(b). Due to the thermal convection induced by body heat, the breathing zone is predominated by the uprising airflow. Therefore, the possibly inhaled contaminant is expected to be delivered from a height lower than the breathing zone. This is constant with many experimental observations and numerical simulations such as those by Rim and Novoselac [7] and Salmanzadeh et al. [20].

For the purpose of model validation, the airflow fields around the manikins in Fig. 1 were compared against the experimental and numerical results available in the literature. Heist et al. [21] measured the airflow field around a child-size thermal manikin (80 cm in height) using PIV technology. In their experiments, the manikin standing with its legs combined was arranged to be back-to-the-wind in a horizontal wind tunnel. In order that hydrodynamic and thermodynamic similarities could be achieved in the computational model with Heist's [21] experimental setup, the combined-leg manikin illustrated in Fig. 1(a) was leeward orientated in the tunnel model and the model boundary conditions were carefully chosen to produce an equal Reynolds number ($Re = 5481$) and Richardson number ($Ri = Ge/Re^2 = 1.27$) with those in the experiments, respectively. Details of the computational procedures could be found in our previous study [1]. The predicted airflow field is compared against Heist's PIV image [21] in Fig. 6. It was found that there is a significant uprising airflow on the downstream side of the manikin, which is a good agreement with the experimental observation.

The airflow field around the manikin with divided legs is compared with Hyun and Kleinstreuer's CFD results [10]. In their simulation, Hyun and Kleinstreuer [10] computed heat transfer from a thermal manikin to a horizontal airflow. The manikin model was facing-the-wind and standing with its legs divided. In order than hydrodynamic and thermodynamic similarities were maintained in the computation, the manikin shown in Fig. 1(b) was arranged to be facing-the-wind and the boundary conditions were carefully chosen. This is the only facing-to-the-wind case in this study. The airflow fields around the manikins are compared in Fig. 7. It was found that the airflow field yielded from this study is in a good agreement with Hyun and Kleinstreuer's numerical result [10]. Similar to what shown in Fig. 6, there was a significant uprising airflow on the downstream side of the manikin. However, the gap between the legs allows airflow in the horizontal direction flowing through it, which leads to a horizontal flow region existing near the floor level and the uprising airflow existing only in the upper region downstream of the manikin.

However, the horizontal flow gets its upward velocity shortly after passing through the leg gap. For the purpose of further

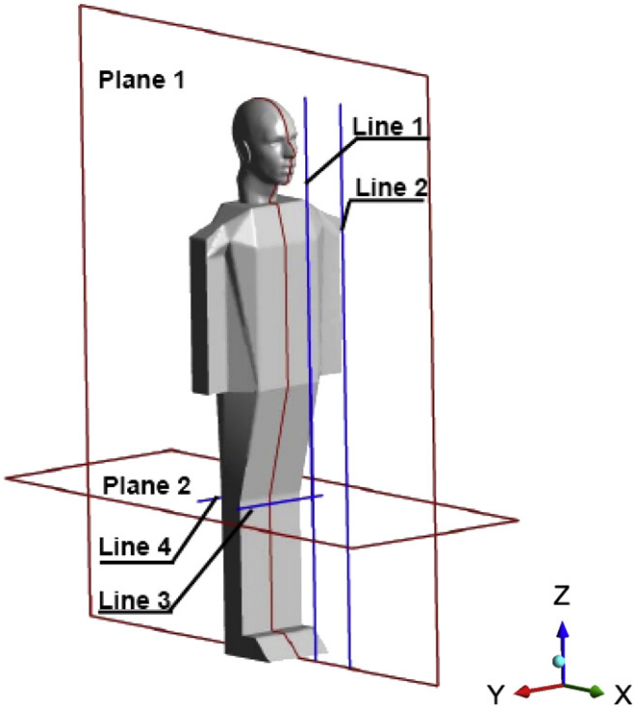

Fig. 4. Locations planes and lines for analysis.

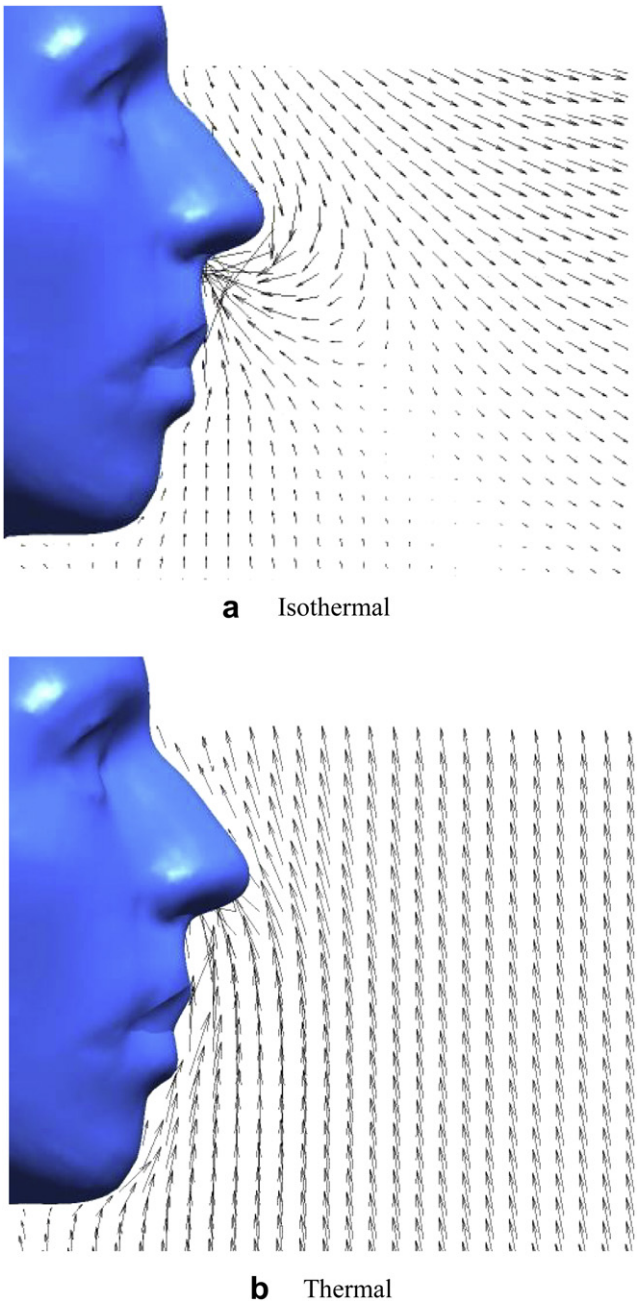

Fig. 5. Airflow vectors in the breathing zone (Plane 1, free stream speed 0.10 m/s).

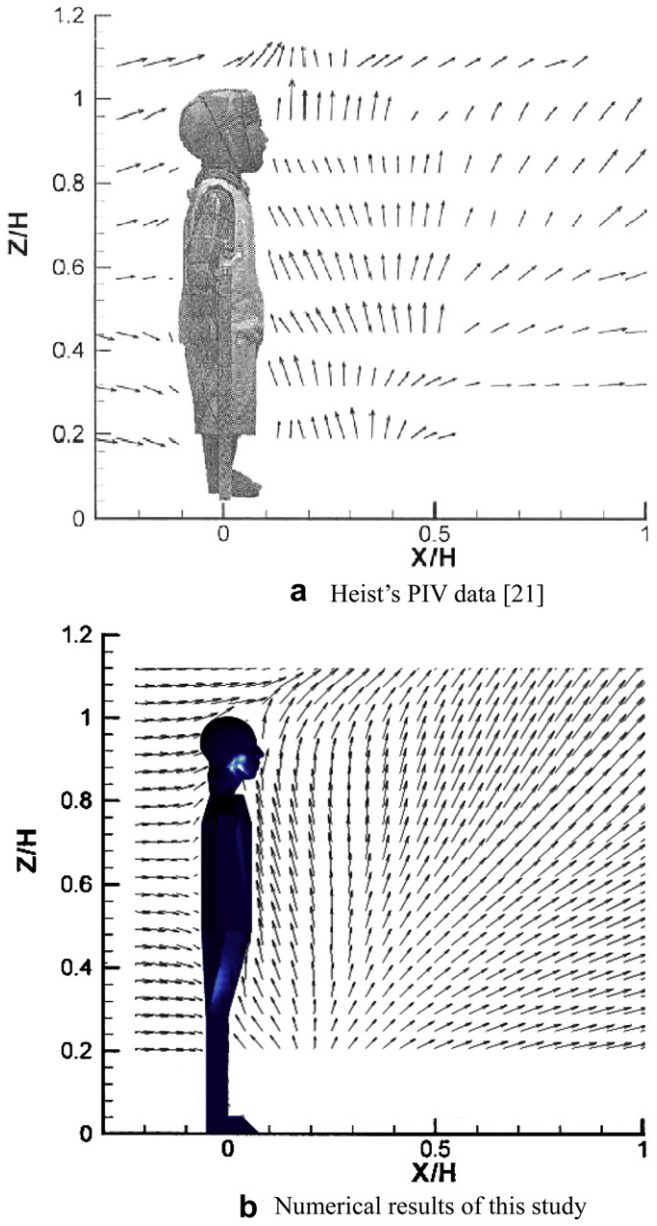

Fig. 6. Comparison of predicted airflow vector plots (Plane 1) against Heist's PIV data [21]. Notes: Thermal manikin with combined legs and back to the wind. Coordinates X and Z are normalized with the manikin height H.

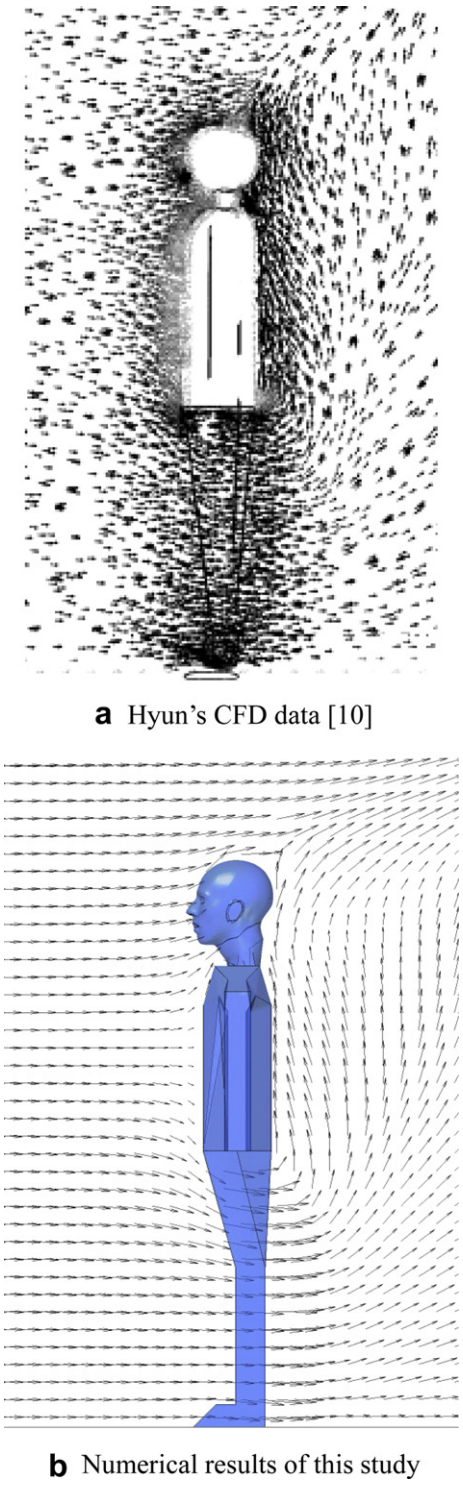

Fig. 7. Comparison of predicted airflow vector plots (Plane 1) against Hyun's CFD data [10]. Notes: Thermal manikin with divided legs and facing the wind.

analysis, the velocity distributions along two vertical lines (Line 1 and 2) are presented in Fig. 8. It was found that when the manikin stands with its legs divided, the W velocity component around the lower body segments ($Z < 0.65$ m) in the downstream vicinity (Line 1) of the manikin is obviously lower than that under the combined-leg condition (Fig. 8(a)). However, this vertical velocity component increases sharply along the Z coordinate so that in the vicinity of the upper body segments the W velocity component becomes larger than that that under the combined-leg situation. The W velocity component under the divided-leg case also has a similar distribution along Line 2 with that of Line 1. However, horizontal airflow flowing through the leg gap leads to a larger airflow velocity within the whole body height range downstream of the manikin. This is especially true in the region around the lower body segments, as shown in Fig. 8(b).

The airflow velocity distributions in Plane 2 around the leg segments under the combined-leg case and the divided-leg case are illustrated in Fig. 9(a) and (b), respectively. It was found that when the legs are combined, there is a big low-velocity vortex region existing at the downstream side of the legs (Fig. 9(a)). When the legs are divided (Fig. 9(b)), there are two vortexes existing on the

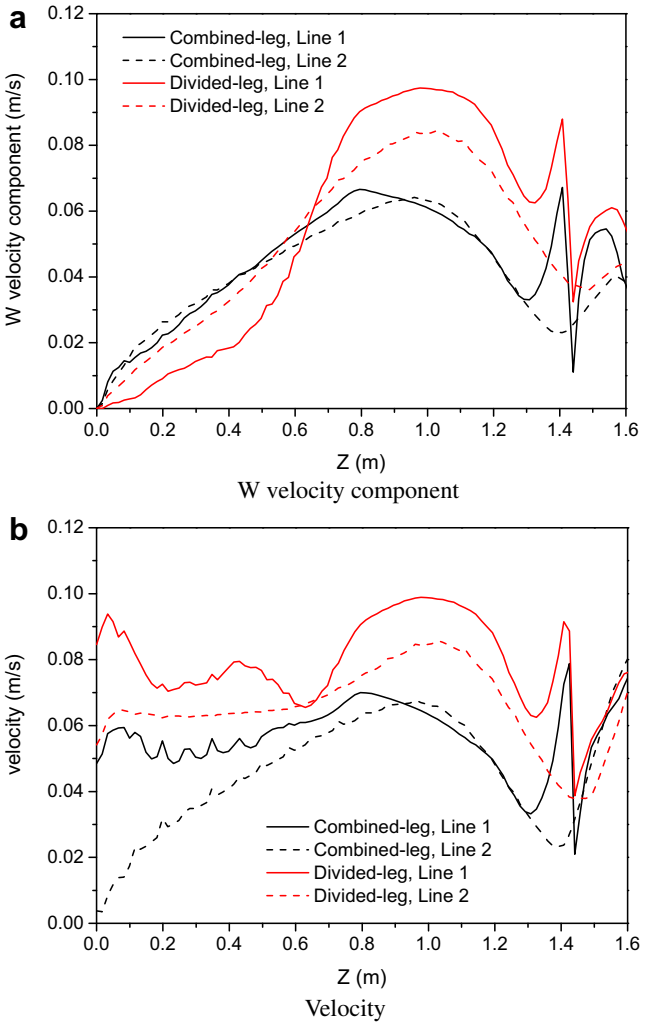

Fig. 8. Velocity distributions along Line 1 and Line 2 (Wind speed 0.10 m/s).

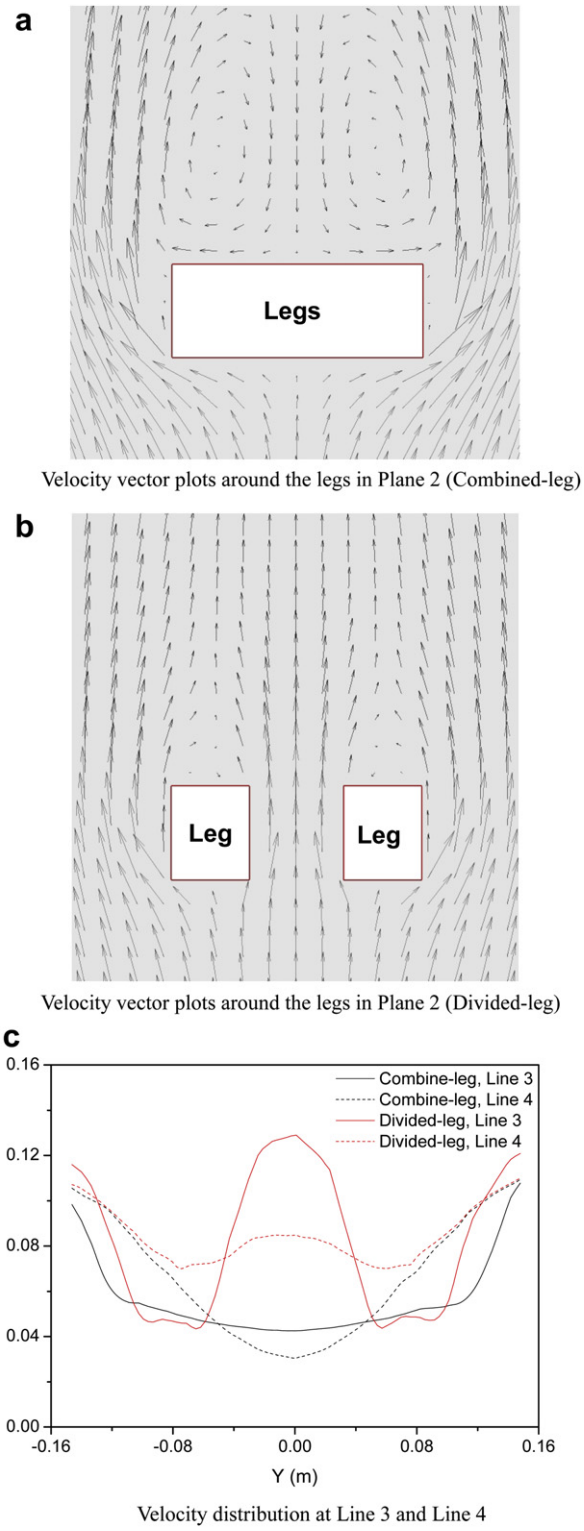

Fig. 9. Air velocity vectors around the leg segments (0.10 m/s).

downstream side of the legs, however, their size is much smaller. The airflow going through the leg gap makes the higher flow intensity on the downstream side the legs. For the purpose of quantitative comparison, the velocity distributions along Line 3 and 4 in Plane 2 (see Fig. 4) are presented in Fig. 9(c). It is clear that the airflow has larger average velocity around the leg segments when the legs are divided.

In brief, the combined legs block the horizontal airflow and cause a strong uprising airflow around the lower body segments, which is capable of contributing to contaminant transport from the floor level into the breathing zone. On the other hand, the divided legs allow a horizontal airflow going through the gap, which not only leads to a larger airflow velocity in the downstream vicinity of the legs, but also leads to a larger vertical velocity component around the upper body segments.

3.2. Heat transfer

The convective heat transfer coefficient between a human body and its surroundings is an important parameter deciding the airflow pattern in the vicinity of the human body as well as the thermal comfort. Since the leg posture is the major focus of this study, the convective heat transfer coefficient of the leg segment is firstly analysed, as shown in Fig. 10. The computations indicated that the divided legs have a higher heat transfer coefficient with the air than the combined ones. Furthermore, the difference in heat transfer coefficient becomes more significant with increasing wind speed. Taking Figs. 8 and 9 into account, the higher heat transfer coefficient with the divided legs should be a result of the higher airflow velocity around the legs.

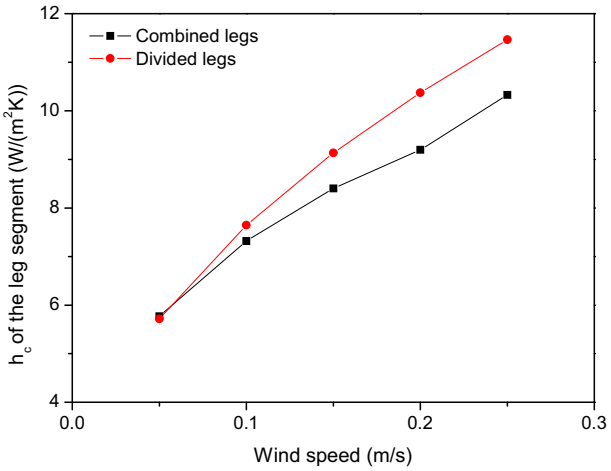

Fig. 10. Convective heat transfer coefficient of the leg segments.

Ishigaki et al. [22] proposed an empirical correlation for the average convective heat transfer coefficient of a human body in a low-speed environment, which takes the form of

$$h_c = 93.7u^{0.257}/(T_s - T_a)^{1.28} \quad 0.05 \le u \le 0.20\ \mathrm{m/s} \tag{1}$$

In addition, Seppanen [23] proposed another correlation to count for the heat transfer of an human occupant in a low-speed environment

$$h_c = \begin{cases} 4.0 & 0 \le u \le 0.15\ \mathrm{m/s} \\ 14.8u^{0.69} & 0.15 \le u \le 1.5\ \mathrm{m/s} \end{cases} \tag{2}$$

In the above equations, u is the environment wind speed and T_s and T_a stand for the human surface temperature and the ambient air temperature, respectively.

Equations (1) and (2) are compared against the predicted heat transfer coefficient in Fig. 11. It is firstly interesting to find out the divided-leg manikin has a larger average heat transfer coefficient than the combined-leg one, which is believed to be a result of the higher airflow velocity (Fig. 8(b)). It is also found that the predicted average heat transfer coefficient agrees well with the Ishigaki's correlation (Equation (1)) when the wind speed is lower than 0.2 m/s. However, the Seppanen correlation (Equation (2)) seems to underpredict the heat transfer coefficient.

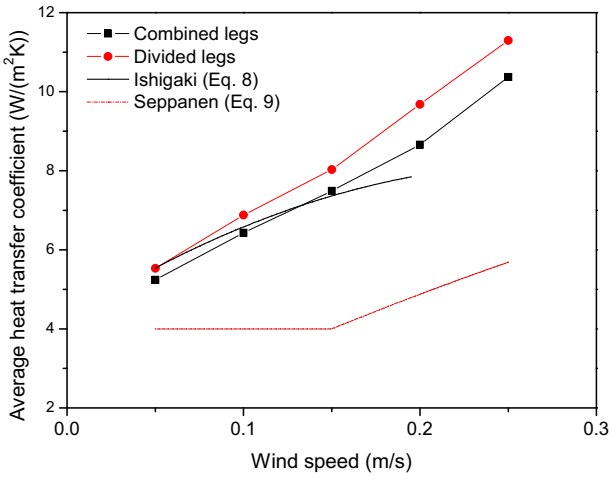

Fig. 11. Comparison of the convective heat transfer coefficient against empirical correlations.

3.3. Particle trajectories

Detailed particle trajectories were also obtained through the computations. Fig. 12 presents typical trajectories of the inhaled particles under different conditions. Fig. 12(a) and (b) present the particle tracks under isothermal conditions. It reveals that for an isothermal flow, the inhaled particles are delivered from a source located slightly lower than the nose height and the particle tracks go around the head. The leg posture thus has no effect on particle inhalation. However, CFD models with heat transfer presented totally different particle trajectories, as shown in Fig. 12(c) and (d). When heat transfer is included in the CFD model, the inhaled particles are observed to be delivered from a source located at a much lower height. Furthermore, it is found that the effect of the leg posture is very significant under the thermal conditions. Fig. 12(c) illustrates that when the manikin stands with its legs combined, the inhaled particles are delivered from a low level near the floor. They pass around the legs from the both sides and then bend their ways upwards sharply. The particles are then transported vertically into the breathing zone by the thermal plume and are finally inhaled. However, Fig. 12(d) indicates that when the legs are divided, the inhaled particles are delivered from a slightly higher level than that in a combined-leg case. Furthermore, the particles go directly through the gap between the legs before bending their paths upward, but do not need to pass around the legs. Bending at higher height also makes the particle trajectories closer to the manikin.

3.4. The critical area

Fig. 12 reveals that the inhaled particles are released from different sources when the flow condition or the leg posture changes. In this study, the concept of "critical area" proposed by Anthony and Flynn [24] is utilized to analyse the source location of inhaled particles. A critical area is a certain area in the particle injection plane ($X = -2$ m plane in the study), particles injected from which are inhaled later by the manikin. The geometrical shape of a critical area may vary largely depending on the flow and thermal conditions as well as the geometrical conditions of the manikin. Our previous study [9] figured out the critical area under the facing-to-the- wind condition takes a water-drop shape, however, this study demonstrated that the critical areas have totally different shapes when the manikin is back-to-the-wind oriented. In addition, this study also demonstrated that the shape and size of a critical area are subjected to the body posture as well.

Typical critical areas under the back-to-the-wind conditions are illustrated in Fig. 13, where the manikin model is also included for the purpose of interpretation. It was found that when the flow is isothermal, the predicted critical area is located slightly lower than the breathing zone. As heat transfer is included in the CFD model, the predicted critical area is not only located at a much lower height, but also highly sensitive to the leg posture. As shown in Fig. 13, when the manikin stands with its legs divided, the critical area is a triangle which takes the shape of the upper leg gap. However, when the manikin legs are combined together, the critical area is located further lower and divided into 2 sub-areas. Actually, the distribution characteristics of critical areas illustrated in Fig. 13 can also be referred to the particle trajectories shown in Fig. 12. When the legs are divided, the gap allows the particles going through it before being inhaled. Meanwhile, size and shape of the gap also have important effects on those of the critical area. When the legs are combined together, since there is no gap for direct

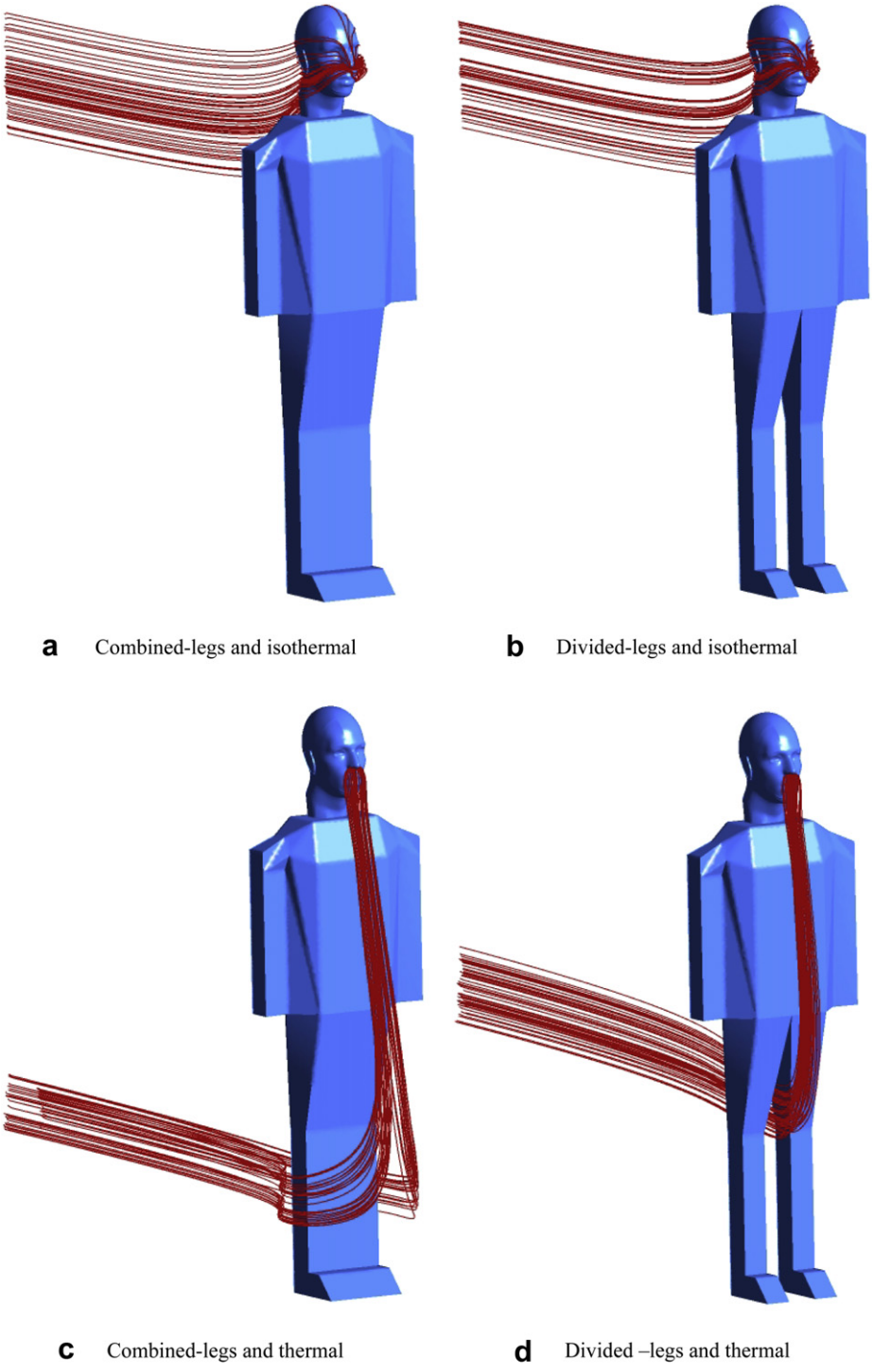

Fig. 12. Typical particle trajectories under various conditions (0.05 m/s).

going-through, particles have to pass around the legs before bending their ways upward.

The central heights of the critical areas are further analysed within the common indoor wind speed range (0.05–0.25 m/s), as shown in Fig. 14. It is firstly found that for the isothermal flows, the two curves for the both leg postures are almost superposed together (See the locally enlarged figure in Fig. 14). This indicates that when heat transfer is not taken into account, the leg posture has no detectable effect on the predicted particle inhalation within the wind speed range considered in this study. However, when heat transfer exists between the manikin and the surrounding air, the effect of leg posture is significant. As shown in Fig. 14, when the manikin stands with its legs combined, the central height of the critical area increases with increasing wind speed. Especially, when the wind speed is over 0.2 m/s, the central height of critical area increases sharply with further increase in the wind speed. As the wind speed reaches 0.25 m/s, the central height of the critical area seems to be the same as that under an isothermal condition. Our

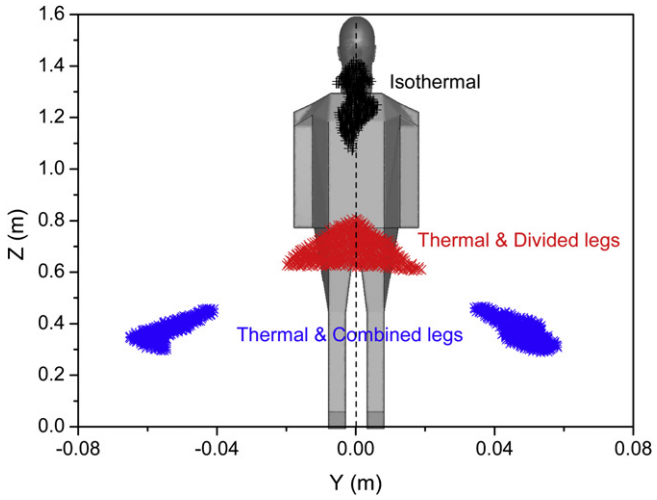

Fig. 13. Typical shapes of the critical areas when the manikin is back to the wind (Wind speed 0.05 m/s). Note: The manikin is included to illustrate the critical area locations relative to the manikin only in the height (*Z*) coordinate. The manikin size in the *Y* coordinate is not proportional with the coordinate scale.

previous study [1] demonstrated that for a leeward manikin with combined legs, the effect of body heat on particle inhalation is gradually suppressed by the increased wind speed. As the wind speed is over 0.2 m/s, particles delivered from both the lower level (those passing around the legs) and the higher level (those passing around the head) are inhaled. As the wind speed reaches up to 0.25 m/s, the effect of body heat could be ignored since particles passing around the legs could no longer be inhaled. This causes the critical area moves upward to the breathing zone height and is very similar to that of an isothermal case shown in Fig. 12(a). However, when the manikin legs are divided, the situation is totally different. It seems that within the wind speed range of this study (0.05–0.25 m/s), the wind speed has no significant effect on the characteristics of particle inhalation despite the central height of critical area slightly decreases with increasing wind speed. Even when the wind speed increases up to 0.25 m/s, the inhaled particles are still delivered from the thigh level.

A comparison of the airflow field and the particle tracks under the higher wind speed (0.25 m/s) may be capable of giving an interpretation to the aforementioned difference. As illustrated in Fig. 15(a), when the manikin stands with its legs combined, there are two reverse-rotating vortexes existing at the downstream side of the manikin. Among them, the lower vortex is entraining particles from near the floor level to a higher level while the upper vortex is delivering particles from the head-top level to a lower level. As the wind speed increases, the upper vortex expands its size and suppresses the lower one. As the wind speed increase up to 0.25 m/s, the size of the upper vortex is large enough and the lower vortex could no longer deliver particles into the breathing zone. However, when the manikin legs are divided, the horizontal airflow through the gap leads to a much larger lower vortex. It was found that this lower vortex expands its size with increasing wind speed and hence intensifies its capability of delivering particles into the breathing zone from the floor level. As a result, within the

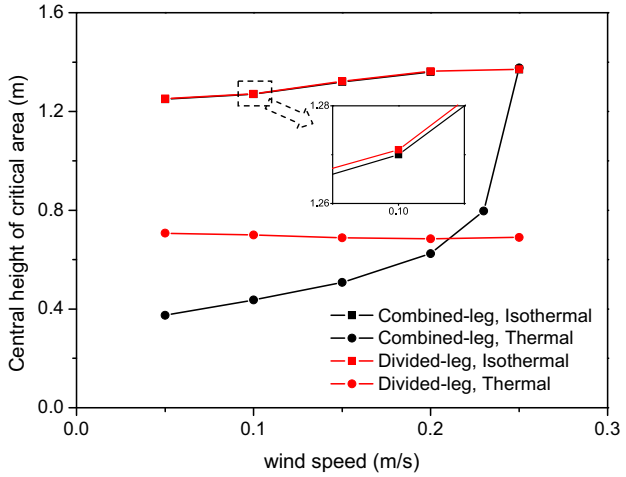

Fig. 14. Central height of the critical area.

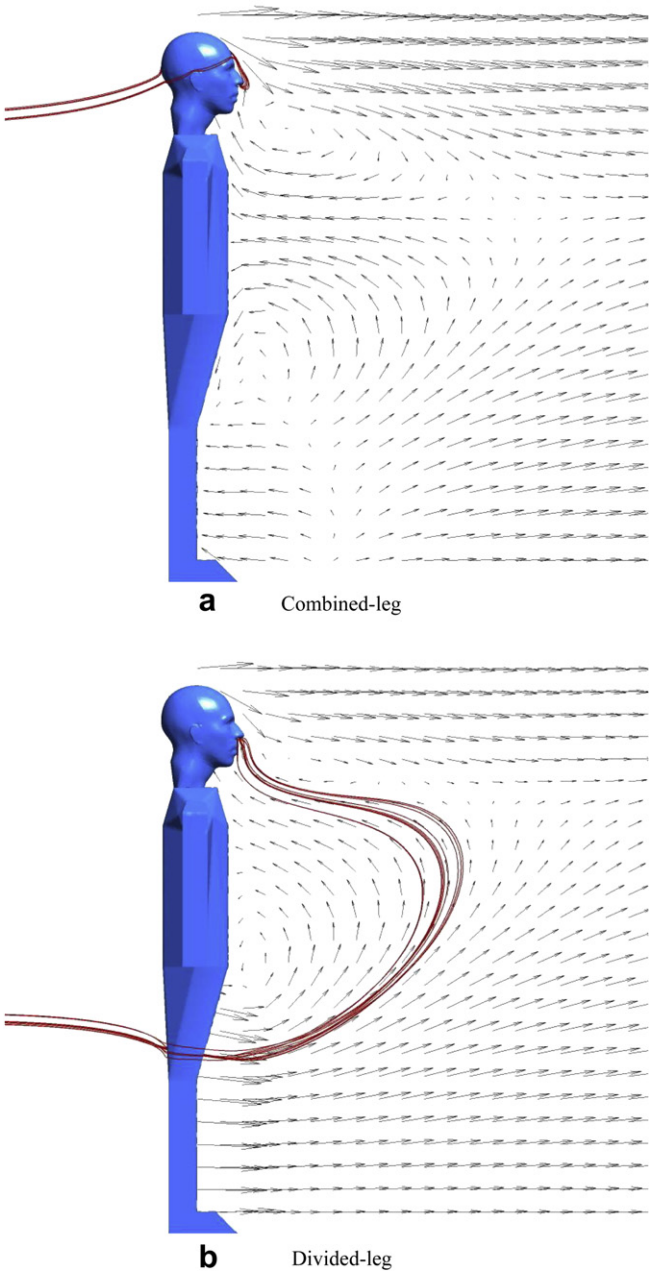

Fig. 15. Comparison of airflow field and particle trajectories (0.25 m/s).

parametric range investigated in this study, the inhaled particles are always delivered from the lower level when the legs are divided.

4. Conclusions

The effects of leg posture (combined legs or divided legs) on the airflow field and particle transport around a thermal manikin standing with its back towards a horizontal free stream were investigated using CFD in this study. The predicted airflow fields and heat transfer coefficient agree well with the published data in the literature. Conclusions rising from this study are as follows:

(1) Divided legs not only allow the free stream flowing through the gap, but also lead to a higher heat transfer intensity around the lower body segments, which causes the uprising airflow around the upper body segments, especially in the breathing zone, has a higher vertical velocity component.
(2) Different leg postures have different environment sensitivity. Within the general indoor wind speed range (0.05–0.25 m/s), the central height of the critical area increases with the wind speed when the legs are combined, and the effects of thermal plume are gradually suppressed. However, when the legs are divided, the increase in the wind speed has no significant effect on the central height of the critical area.

Acknowledgements

The financial supports provided by the National Basic Research Program (973) of China (Grant No. 2012CB720100), the Australian Research Council (project ID LP110100140) and the Natural Science Foundation of China (Grant No. 21277080) are gratefully acknowledged.

References

[1] Ge QJ, Li XD, Inthavong K, Tu JY. Numerical study of the effects of human body heat on particle transport and inhalation in indoor environment. Build Environ 2013;59:1–9.
[2] Homma H, Yakiyama M. Examination of free convection around occupant's body caused by its metabolic heat. ASHRAE Trans 1988;94:104–24.
[3] Johnson AE, Fletcher B, Saunders CJ. Air movement around a worker in a low-speed flow field. Ann Occup Hyg 1996;40:57–64.
[4] Craven BA, Settles GS. A computational and experimental investigation of the human thermal plume. J Fluid Eng Trans ASME 2006;128:1251–8.
[5] Baldwin PEJ, Maynard AD. A survey of wind speeds in indoor workplaces. Ann Occup Hyg 1998;42:303–13.
[6] Zukowska D, Popiolek Z, Melikov A. Impact of personal factors and furniture arrangement on the thermal plume above a human body. In: Proceedings of the 10th international conference on air distribution in rooms – Roomvent 2007. Helsinki, Finland; 2007. p. 137–44.
[7] Rim D, Novoselac A. Transport of particulate and gaseous pollutants in the vicinity of a human body. Build Environ 2009;44:1840–9.
[8] Longest PW, Kleinstreuer C, Buchanan JR. Efficient computation of micro-particle dynamics including wall effects. Comput Fluids 2004;33:577–601.
[9] Se CMK, Inthavong K, Tu JY. Inhalability of micron particles through the nose and mouth. Inhal Toxicol 2010;22:287–300.
[10] Hyun S, Kleinstreuer C. Numerical simulation of mixed convection heat and mass transfer in a human inhalation test chamber. Int J Heat Mass Transf 2001;44:2247–60.
[11] Kurazumi Y, Tsuchikawa T, Ishii J, Fukagawa K, Yamato Y, Matsubara N. Radiative and convective heat transfer coefficients of the human body in natural convection. Build Environ 2008;43:2142–53.
[12] Hayashi T, Ishizu Y, Kato S, Murakami S. CFD analysis on characteristics of contaminated indoor air ventilation and its application in the evaluation of the effects of contaminant inhalation by a human occupant. Build Environ 2002;37:219–30.
[13] Brohus H, Nielsen PV. CFD models of persons evaluated by full-scale wind channel experiments. Proceedings of Roomvent 96. Yokohama, Japan; 1996. p. 137–44.
[14] Murakami S, Kato S, Zeng J. Combined simulation of airflow, radiation and moisture transport for heat release from a human body. Build Environ 2000; 35:489–500.
[15] Gao NP, Niu JL. CFD study of the thermal environment around a human body: a review. Indoor Built Environ 2005;14:5–16.
[16] Tilley AR. The measure of man and woman. New York: The Whitney Library of Design; 1993.
[17] Gao N, Niu J. CFD study on micro-environment around human body and personalized ventilation. Build Environ 2004;39:795–805.
[18] Sorensen DN, Voigt LK. Modelling flow and heat transfer around a seated human body by computational fluid dynamics. Build Environ 2003;38: 753–62.
[19] Li XD, Inthavong K, Tu JY. Particle inhalation and deposition in a human nasal cavity from the external surrounding environment. Build Environ 2012;47: 32–9.
[20] Salmanzadeh M, Zadedi G, Ahmadi G, Marr DR, Glauser M. Computational modeling of effects of thermal plume adjacent to the body on the indoor airflow and particle transport. J Aerosol Sci 2012;53:29–39.
[21] Heist DK, Eisner AD, Mitchell W, Wiener R. Airflow around a child-size manikin in a low-speed wind environment. Aerosol Sci Technol 2003;37: 303–14.
[22] Ishigaki H, Horikoshi T, Uematsu T, Sahashi M, Tsuchikawa T, Mochida T, et al. Experimental-study on convective heat-transfer coefficient of the human-body. J Therm Biol 1993;18:455–8.
[23] Seppanen O. Thermal insulating values for typical indoor clothing ensembles. ASHRAE Trans 1972;78:120–30.
[24] Anthony TR, Flynn MR. Computational fluid dynamics investigation of particle inhalability. J Aerosol Sci 2006;37:750–65.